Nonlocal characteristics of two-qubit gates and their argand diagrams

M. Karthick Selvan* and S. Balakrishnan†
Department of Physics, School of Advanced Sciences,
Vellore Institute of Technology, Vellore - 632014, Tamilnadu, India.

In this paper, we show the usefulness of the chords present in the argand diagram of squared eigenvalues of nonlocal part of two-qubit gates to study their nonlocal characteristics. We discuss about the criteria for perfect entanglers to transform a pair of orthonormal product states into a pair of orthonormal maximally entangled states. Perfect entanglers with a chord passing through origin can do such a transformation. We show that all the perfect entanglers with at least one chord passing through origin form five different planes of Weyl chamber. Perfect entanglers represented by each plane have unique entangling characteristics. We also provide the conditions for a perfect entangler not present in one of those five planes to transform a pair of orthonormal product states into orthonormal maximally entangled states. Finally, we show that similar to entangling power, gate typicality can also be described using the chords present in the argand diagram. For each chord describing the entangling power there exists a chord describing the gate typicality. We show the geometrical relation between the two sets of chords.

arXiv:2502.03820v1 [quant-ph] 6 Feb 2025

I. INTRODUCTION

Understanding the geometry and nonlocal characteristics of two-qubit gates is essential as their role in quantum computation is vital [1–3]. Over two decades, two-qubit gates have been studied vastly. Nonlocal characteristics of two-qubit gates are invariant under local operations. A complete set of local invariants of two-qubit gates were obtained in [4]. The geometry of local equivalence classes of two-qubit gates was studied in detail in [5]. A measure for operator entanglement was introduced in [6]. Nonlocal characteristics of two-qubit gates were considered as resources for doing quantum information processing and their quantification was studied in [7]. Entangling power, a quantity to measure the ability of two-qubit gates to generate entanglement, was defined in [8]; its expression in terms of Cartan co-ordinates [9] and local invariants [10] were derived. Gate typicality as complementary to entangling power was introduced [11] and its properties for two-qubit gates were studied [12].

Despite many studies, still there remains unexplored ways to understand the nonlocal characteristics of two-qubit gates. Recently, the chords present in the argand diagram of squared eigenvalues of nonlocal parts of two-qubit gates were shown to describe the ability of two-qubit gates to generate entangled states [13]. This argand diagram was studied in regard to the condition for perfect entanglers [4, 5], operational discrimination of nonlocal part of a two-qubit gate from the nonlocal part of its adjoint [14], and simulation of perfect entanglers [15]. Perfect entanglers are two-qubit gates that can transform some product state into a maximally entangled state. For perfect entanglers, convex hull of squared eigenvalues of their nonlocal part contains zero [4, 5]. Among perfect entanglers, special perfect entanglers (SPEs) can transform orthonormal product basis into orthonormal maximally entangled basis [9]. Recently, it was shown that perfect entanglers with a chord passing through origin in their argand diagram can transform a pair of orthonormal product states into a pair of orthonormal maximally entangled states [13]. Now, there ariases a question that can a perfect entangler without any chords passing through origin transform a pair of orthonormal product states into a pair of orthonormal maximally entangled states?

In this paper, we provide answer to this question. First, we identify the regions of perfect entanglers with at least one chord passing through origin. Next, we derive three sets of orthogonal conditions, in terms of eigenvalues of generators of perfect entanglers, between a pair of product states obtained from the argand diagram of perfect entanglers without any chord passing through origin. A perfect entangler without any chord passing through origin and transforming a pair of orthonormal product states into maximally entangled states should satisfy one of those conditions. We also provide an example for existence of such perfect entanglers. Finally, we show that in addition to entangling power, the chords present in the argand diagram can also be used to quantify the gate typicality and linear entropy [6] of two-qubit gates.

II. BACKGROUND

A two-qubit gate $U \in \mathrm{SU}(4)$ can be decomposed as follows [5].

$$U = L_1 U_d(c_x, c_y, c_z) L_2, \tag{1}$$

where $L_1,\ L_2 \in \mathrm{SU}(2) \otimes \mathrm{SU}(2)$ are local parts of U and $U_d(c_x, c_y, c_z)$ is the nonlocal part of U. Two-qubit gates having the same nonlocal part but differing only in the local parts form a local equivalence class and each local equivalence class of two-qubit gates are geometrically represented as a point of tetrahedron shown in FIG. 1.

* karthick.selvan@yahoo.com
† physicsbalki@gmail.com

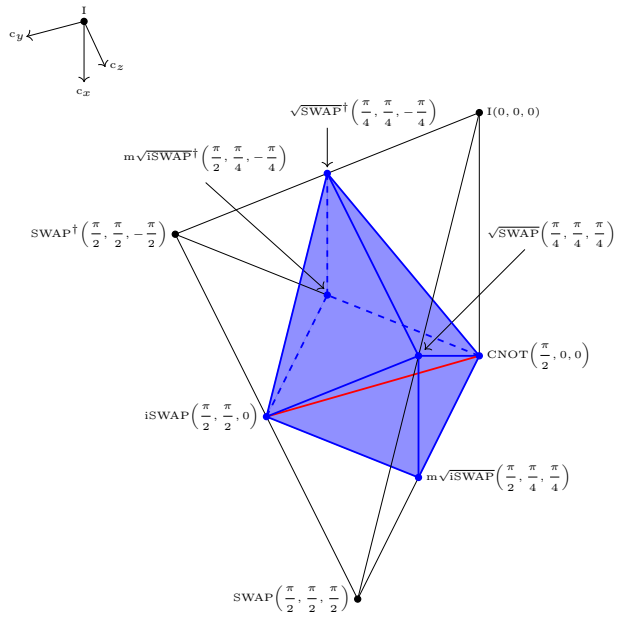

FIG. 1. Geometry of local equivalence classes of two-qubit gates. Region colored in blue is the region of perfect entanglers. The line in red color represent special perfect entanglers.

Nonlocal characteristics of U is determined by its nonlocal part which can be written as

$$U_d(c_x, c_y, c_z) = e^{iH/2} \tag{2}$$

with

$$H = \sum_{j=x,y,z} c_j \left(\sigma_j \otimes \sigma_j\right), \tag{3}$$

where c_x, c_y, c_z are called Cartan co-ordinates. Eigenvalues of H are given by

$$h_1 = c_x - c_y + c_z,$$

$$h_2 = c_x + c_y - c_z,$$

$$h_3 = -c_x - c_y - c_z,$$

and

$$h_4 = -c_x + c_y + c_z. \tag{4}$$

Eigen decomposition of the nonlocal part of U can be written as shown below.

$$U_d(c_1, c_2, c_3) = \frac{1}{2}\sum_{j=1}^{4} e^{ih_j/2}|\Psi_j\rangle\langle\Psi_j|, \tag{5}$$

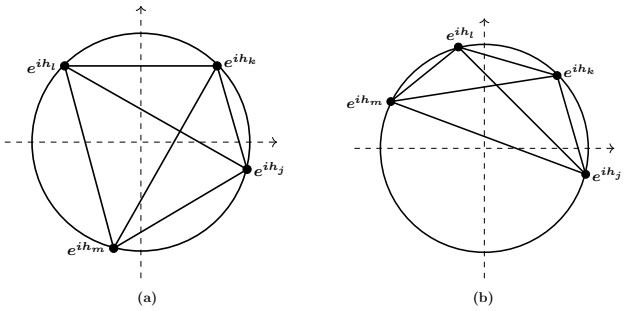

FIG. 2. Argand diagram of squared eigenvalues of (a) a perfect entangler, and (b) a non perfect entangler.

where $|\Psi_j\rangle$'s are unnormalized vectors forming the eigen basis of U_d. It is also called as magic basis [5] and the expressions of unnormalized vectors are given below.

$$|\Psi_1\rangle = \begin{bmatrix}1\\0\\0\\1\end{bmatrix},\ |\Psi_2\rangle = \begin{bmatrix}0\\i\\i\\0\end{bmatrix}, |\Psi_3\rangle = \begin{bmatrix}0\\1\\-1\\0\end{bmatrix},\ |\Psi_4\rangle = \begin{bmatrix}i\\0\\0\\-i\end{bmatrix}. \tag{6}$$

The squared eigenvalues of U_d are on a circle of unit radius in the complex plane and they are pairwise connected by six chords forming a quadrilateral as shown in FIG. 2. We refer to this argand diagram of squared eigenvalues of U_d as the argand diagram of U.

The Cartan co-ordinates of perfect entanglers which can transform a product state into a maximally entangled state satisfy the following conditions [16].

$$c_x + c_y \geq \frac{\pi}{2},$$

$$c_y \pm c_z \leq \frac{\pi}{2}. \tag{7}$$

The region of perfect entanglers (colored in blue) is shown in FIG. 1. Special perfect entanglers which are perfect entanglers with maximum entangling power [9] is represenetd by the red color line in FIG. 1. For perfect entanglers, the convex hull of squared eigenvalues of U_d encloses zero. The argand diagram of a typical perfect entangler (non perfect entangler) is shown in FIG. 2a (FIG. 2b).

III. PERFECT ENTANGLERS WITH CHORDS PASSING THROUGH ORIGIN

In this section, we identify the regions of perfect entanglers with at least one chord passing through origin. The chord connecting e^{ih_j} and e^{ih_k} passes through origin only if $|h_j - h_k| = \pi$. It can be verified that the equations $|h_j - h_{j+1}| = \pi$ with $j = 1, 2, 3$ describe the three

boundary planes separating perfect entanglers from non perfect entanglers inside the Weyl chamber [Eq. 7]. These three planes are shown in FIG. 3a. Similarly, the equations $|h_j - h_{j+2}| = \pi$ with $j = 1, 2$ describe the planes $c_x \pm c_z = \pi/2$ [FIG. 3b]. These two planes together form one of the reflecting plane, $c_x + \text{sign}(c_z)c_z = \pi/2$, describing the mirror operation [17]. The equation $|h_1 - h_4| = \pi$ which can be rewritten as $c_x - c_y = \pi/2$ is satisfied only by the point representing CNOT equivalence class. Thus only the gates represented by the five planes shown in FIG. 3a and FIG. 3b have atleast one chord passing through origin and hence they can transform a pair of orthonormal product states into a pair of orthonormal maximally entangled states.

All the gates represented by a specific plane have unique argand diagram with a specific chord passing through origin. However, there are gates present in more than one plane. SPEs are at the intersection of $|h_j - h_{j+2}| = \pi$ $(j = 1, 2)$ planes. Hence, for SPEs, two chords connecting diametrically opposite points (e^{ih_j} and $e^{ih_{j+2}}$ with $j = 1, 2$) pass through origin and they can transform an orthonormal product basis into orthonormal maximally entangled basis [9, 13]. Among SPEs, the point representing iSWAP equivalence class is also present in $|h_j - h_{j+1}| = \pi$ with $j = 1, 3$ planes. Similarly, the point representing CNOT equivalence class also satify the conditions, $|h_2 - h_3| = \pi$ and $|h_1 - h_4| = \pi$. Hence, these two equivalence classes have argand diagrams with four chords passing through origin [13].

Similar to SPEs, there are local equivalence classes at the intersection of two planes: between the pairs of planes $(|h_3 - h_4| = \pi, |h_1 - h_3| = \pi)$, $(|h_2 - h_3| = \pi, |h_1 - h_3| = \pi)$, $(|h_1 - h_2| = \pi, |h_2 - h_4| = \pi)$, and $(|h_2 - h_3| = \pi, |h_2 - h_4| = \pi)$. However, for these equivalence classes, the two chords connecting diametrically opposite points do not pass through origin but, only one of them pass through origin. Hence these equivalence classes cannot transform a orthonormal product basis into orthonormal maximally entangled basis.

The point representing $\sqrt{\text{SWAP}}$ equivalence class is common to $|h_3 - h_4| = \pi$, $|h_1 - h_3| = \pi$, and $|h_2 - h_3| = \pi$ planes. Hence, in the argand diagram of $\sqrt{\text{SWAP}}$ equivalence class, three chords from the point e^{ih_3} pass through origin. It implies that the remaining three points e^{ih_1}, e^{ih_2}, and e^{ih_4} coincide with each other and the argand diagram has only three chords. Similarly, it can be verified that the argand diagram of $\sqrt{\text{SWAP}}^\dagger$ equivalence class has only three chords from the point e^{ih_2} passing through origin. Thus for the gates belonging to these two equivalence classes there exist three different pairs of orthonormal product states that can be transformed into pairs of orthonormal maximally entangled states.

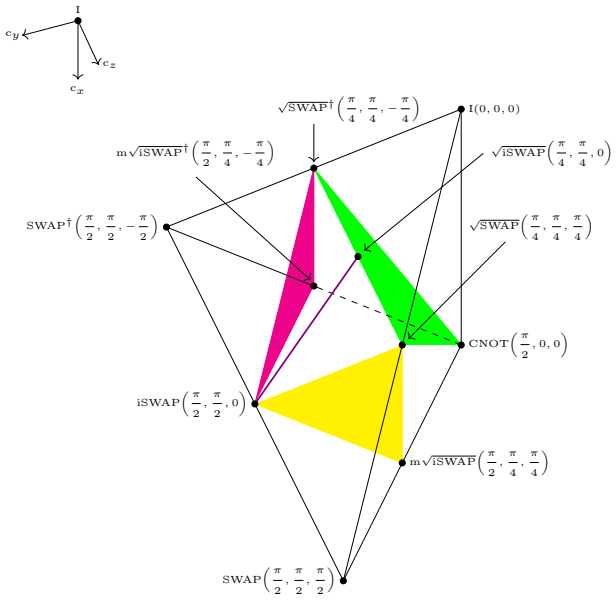

(a)

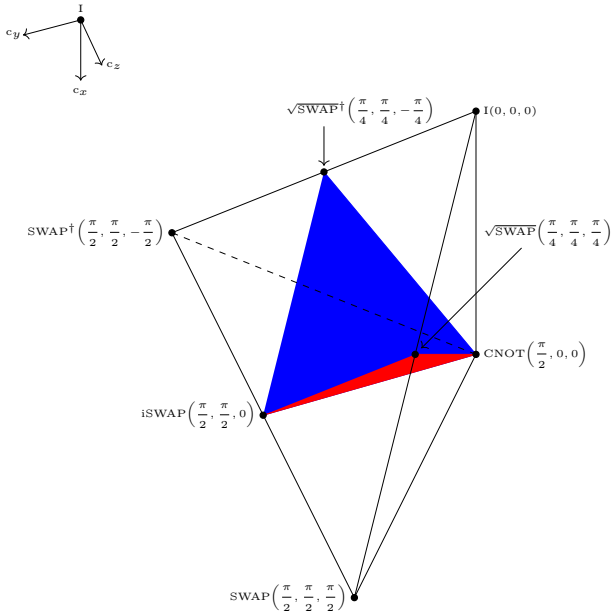

(b)

FIG. 3. Regions of perfect entanglers with at least one chord passing through origin. In the subfigure (a) the planes colored in meganta, green, and yellow are $|h_1 - h_2| = \pi$, $|h_2 - h_3| = \pi$, and $|h_3 - h_4| = \pi$ planes respectively. The violet line (excluding the end points) represents perfect entanglers without any chord passing through origin but capable of transforming a pair of orthonormal product states into a maximally entangled states. In the subfigure (b), the planes colored in red and blue are $|h_1 - h_3| = \pi$ and $|h_2 - h_4| = \pi$ planes respectively.

IV. PAIR OF ORTHONORMAL PRODUCT STATES TO MAXIMALLY ENTANGLED STATES

In this section, we consider the perfect entanglers existing in other regions. A typical argand diagram of perfect entanglers is shown in FIG. 2a. In FIG. 2a, the origin is contained in two triangles: the triangle with vertices e^{ih_j}, e^{ih_l}, and e^{ih_m}, and the triangle with vertices e^{ih_k}, e^{ih_l}, and e^{ih_m}. Hence, there exist two sets of weights or co-ordinates such that

$$|\phi_j|^2 e^{ih_j} + |\phi_l|^2 e^{ih_l} + |\phi_m|^2 e^{ih_m} = 0, \tag{8}$$

and

$$|\phi'_k|^2 e^{ih_k} + |\phi'_l|^2 e^{ih_l} + |\phi'_m|^2 e^{ih_m} = 0, \tag{9}$$

with $|\phi_j|^2+|\phi_l|^2+|\phi_m|^2 = 1$ and $|\phi'_k|^2+|\phi'_l|^2+|\phi'_m|^2 = 1$. From Eqs. 8 and 9, following two product states can be constructed [5].

$$|\Phi_1\rangle = |\phi_j|e^{-i(a\pi+h_j/2)}|\Psi_j\rangle + |\phi_l|e^{-i(b\pi+h_l/2)}|\Psi_l\rangle + |\phi_m|e^{-i(c\pi+h_m/2)}|\Psi_m\rangle, \tag{10}$$

and

$$|\Phi_2\rangle = |\phi'_k|e^{-i(d\pi+h_k/2}|\Psi_k\rangle + |\phi'_l|e^{-i(f\pi+h_l/2)}|\Psi_l\rangle + |\phi'_m|e^{-i(g\pi+h_m/2)}|\Psi_m\rangle, \tag{11}$$

for some integers $a, b, c, d, f,$ and g. Now we consider the following cases.

Case 1: First, we derive the condition for the existence of a pair of orthonormal product states with respect to a triangle enclosing the origin. For example, in FIG. 2a, we consider the triangle with vertices e^{ih_j}, e^{ih_l}, and e^{ih_m}. A product state corresponding to this triangle is given in Eq. 10. Now we construct another product state with respect to the same triangle, for some integers $a', b',$ and c', as shown below.

$$|\Phi'_1\rangle = |\phi_j|e^{-i(a'\pi+h_j/2)}|\Psi_j\rangle + |\phi_l|e^{-i(b'\pi+h_l/2)}|\Psi_l\rangle + |\phi_m|e^{-i(c'\pi+h_m/2)}|\Psi_m\rangle. \tag{12}$$

These two product states, $|\Phi_1\rangle$ and $|\Phi'_1\rangle$, can be converted into maximally entangled states by $U_d(c_1, c_2, c_3)$. These two states to be orthogonal the following condition needs to be satisfied.

$$|\phi_j|^2 e^{i(a'-a)\pi} + |\phi_l|^2 e^{i(b'-b)\pi} + |\phi_m|^2 e^{i(c'-c)\pi} = 0. \tag{13}$$

This condition will be satisfied only if either one of $(a'-a)$, $(b'-b)$, and $(c'-c)$ is even (odd) and other two are odd (even). If $(a'-a)$ is chosen as even (odd) and the other two as odd (even), then we get

$$|\phi_j|^2 = |\phi_l|^2 + |\phi_m|^2. \tag{14}$$

Along with normalization, it can be found that $|\phi_j|^2 = 1/2$. Thus, to construct a pair of orthonormal product states with respect to the triangle formed by e^{ih_j}, e^{ih_l}, and e^{ih_m}, one of the weights in Eq. 8 should be 1/2. The condition for $|\phi_j|^2 = 0.5$, can be written in terms of eigenvalues of H as follows.

$$\frac{2|\cos h_k \sin h_l - \cos h_l \sin h_k|}{|\cos h_j(\sin h_k - \sin h_l) + \cos h_k(\sin h_l - \sin h_j) + \cos h_l(\sin h_j - \sin h_k)|} = 1. \tag{15}$$

Similar conditions can also be written for other two weights $|\phi_l|^2$ and $|\phi_m|^2$.

Case 2: Now, we consider the case where e^{ih_j} coincides with e^{ih_k} in FIG. 2a. In this case, we have $|\phi'_k| = |\phi_j|$, $|\phi'_l| = |\phi_l|$, and $|\phi'_m| = |\phi_m|$ in Eqs. 9 and 11. Choosing $(f-b)$ as even (odd) and $(g-c)$ as odd (even), the orthogonalization condition becomes

$$|\phi_l|^2 = |\phi_m|^2. \tag{16}$$

This condition can be expressed in terms of eigenvalues of H as follows.

$$\frac{|\cos h_m \sin h_j - \cos h_j \sin h_m|}{|\cos h_j \sin h_l - \cos h_l \sin h_j|} = 1. \tag{17}$$

Case 3: Now, we derive the condition for the two product states shown in Eqs. 10 and 11 to be orthogonal. These two product states correspond to the two triangles containing the origin in FIG. 2a. The condition for orthogonalization between those two product states can be written as follows.

$$|\phi_l||\phi'_l|e^{i(f-b)\pi} = -|\phi_m||\phi'_m|e^{i(g-c)\pi}. \tag{18}$$

Above equation can be rearranged after taking square on both sides as follows.

$$\frac{|\phi_l|^2}{|\phi_m|^2} = \frac{|\phi'_m|^2}{|\phi'_l|^2}. \tag{19}$$

This condition can be expressed in terms of the eigenvalues of H as follows.

$$\frac{|\cos h_m \sin h_j - \sin h_m \cos h_j|}{|\sin h_l \cos h_j - \cos h_l \sin h_j|} = \frac{|\sin h_l \cos h_k - \cos h_l \sin h_k|}{|\cos h_m \sin h_k - \sin h_m \cos h_k|}. \tag{20}$$

Thus, if the eigenvalues of H satisfy the above condition, then it is possible to construct a pair of orthonormal product states that can be converted into a pair of orthonormal maximally entangled states by the perfect entangler $e^{iH/2}$ with the argand diagram shown in FIG. 2a.

To show that there exist perfect entanglers without any chord passing through origin but, capable of transforming a pair of orthonormal product states into maximally entangled states, we consider the triangular region with vertices $(\pi/4, \pi/4, \pm\pi/4)$ and $(\pi/2, \pi/2, 0)$ in the Weyl chamber [FIG. 3a]. It is a region of perfect entanglers with $h_1 = h_4$. For perfect entanglers represented by the edges of the triangle at least one chord passes through origin and for those represented by the interior points only the conditions given in cases 1 and 2, discussed above, are applicable. It can be verified that the conditions ($|\phi_1|^2 = 0.5, |\phi_2|^2 = 0.5,$ and $|\phi_3|^2 = 0.5$) described in case 1 are not satisfied by any perfect entanglers represented by the interior points and only the line connecting $\sqrt{\text{iSWAP}}$ and iSWAP [FIG. 3a] satisfy the condition ($|\phi_2|^2 = |\phi_3|^2$) described in case 2. Thus, in this perfect entanglers region without any chord passing through origin, only the perfect entanglers represented by the violet colored line (shown in FIG. 3) can transform a pair of orthonormal product states into maximally entangled states and the perfect entanglers represented by other interior points cannot do such a transformation.

V. QUANTIFICATION OF NONLOCAL CHARACTERISTICS USING CHORDS

Like two-qubit states, two-qubit gates also possess entanglement and it can be quantified using linear entropy [6, 18]. Two-qubit gates represented by c_3 axis of Weyl chamber have maximum value of linear entropy [19]. Entangling power is another nonlocal measure of two-qubit gates which quantifies the average entanglement generated over uniform distribution of product states [8, 9]. Gate typicality is a nonlocal measure which is complementary to entangling power [11, 12]. Both entangling power (e_p) and gate typicality (g_t) together describe the linear entropy (L) of two-qubit gates. The relationship between them can be written as follows.

$$L = \frac{3}{8}\left[3e_p + g_t\right]. \tag{21}$$

Recently, entangling power of two-qubit gates was shown to be proportional to mean squared length of the chords in the argand diagram of two-qubit gates [13]. Entangling power can be written in terms of chord lengths as follows.

$$e_p = \frac{1}{72}\sum_{j=1}^{3}\sum_{k>j}|e^{ih_j} - e^{ih_k}|^2. \tag{22}$$

Entangling power of a two-qubit gate U can also be expressed as symmetric combination of $L(U)$ and $L(US) - L(S)$ as follows [11, 18, 19].

$$e_p(U) = \frac{4}{9}\left(L(U) + [L(US) - L(S)]\right), \tag{23}$$

where $L(U)$, $L(US)$, and $L(S)$ are linear entropies of the two-qubit gate U, its mirror gate, and SWAP gate respectively.

Gate typicality of a two-qubit gate U was defined as antisymmetric combination of $L(U)$ and $L(US) - L(S)$ [11].

$$g_t(U) = \frac{4}{3}\left(L(U) - [L(US) - L(S)]\right). \tag{24}$$

It can be noted that six times the right hand side of Eq. 22 with e^{ih_k} replaced by its complex conjugate provides the expression of gate typicality of two-qubit gates. That is,

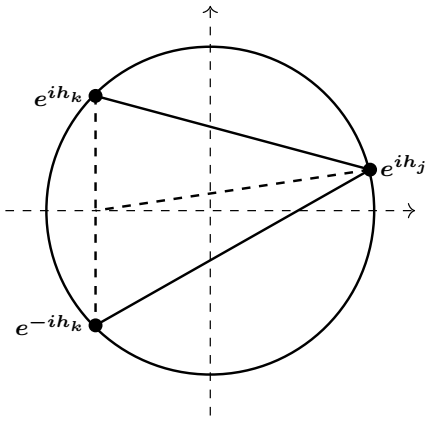

FIG. 4. Diagram explaining the geometrical relation between $|e^{ih_j} - e^{ih_k}|$ and $|e^{ih_j} - e^{-ih_k}|$.

$$g_t = \frac{1}{12}\sum_{j=1}^{3}\sum_{k>j}|e^{ih_j} - e^{-ih_k}|^2. \tag{25}$$

This replacement of e^{ih_k} by its complex conjugate in Eq. 22 can be geometrically interpreted as follows: All the three points e^{ih_j}, e^{ih_k}, and e^{-ih_k} in the argand diagram define a triangle as shown in FIG. 4. The side connecting e^{ih_k} and e^{-ih_k} is parallel to the imaginary axis. The side connecting e^{ih_j} and e^{ih_k}, and the side connecting e^{ih_j} and e^{-ih_k} are reflection of each other about the median from e^{ih_j}. We refer to the chord connecting e^{ih_j} and e^{-ih_k} as the median reflected chord corresponding to the chord connecting e^{ih_j} and e^{ih_k}. For each chord defining entangling power (shown in FIG. 2a) their corresponding median reflected chords define gate typicality. Thus, replacing the symmetric combination of $L(U)$ and $L(US) - L(S)$ in the definition of entangling power by its antisymmetric combination to define gate typicality corresponds to replacing the squared length of the chords describing the entangling power by the squared length of their corresponding median reflected chords. It has to be noted that if any chord describing the entangling power is parallel to imaginary axis, then the length of the corresponding chord describing the gate typicality is zero.

Gate typicality can also be described using only three median reflected chords as shown below.

$$g_t = \frac{1}{6}\sum_{k\neq j}|e^{ih_j} - e^{-ih_k}|^2, \quad \text{for any } j. \tag{26}$$

However, the expression of gate typicality given in Eq. 25 has the same form as the expression of entangling power. Hence, it is useful to describe the difference between the mathematical definitions of entangling power and gate typicality.

Since both entangling power and gate typicality of a two-qubit gate can be calculated using the chords present in their argand diagram, the linear entropy (Eq. 21) describing the operator entanglement of the two-qubit gate can also be calculated using the chords as follows.

$$L = \frac{1}{64}\sum_{j=1}^{3}\sum_{k>j}\left[|e^{ih_j} - e^{ih_k}|^2 + 2|e^{ih_j} - e^{-ih_k}|^2\right] \tag{27}$$

VI. CONCLUSION

To conclude, the argand diagram of squared eigenvalues of nonlocal part of two-qubit gates are very useful to calculate the nonlocal measures such as entangling power, gate typicality, and operator entanglement of two-qubit gates. In the argand diagram of a two-qubit gate, for each chord describing the entangling power, there exist a median reflected chord describing the gate typicality. We have identified the planes containing the perfect entanglers with chords passing through origin. Among SPEs, only the points representing CNOT and iSWAP equivalence classes are present in more than two planes and all other SPEs are contained in two planes. $\sqrt{\text{SWAP}}$ and $\sqrt{\text{SWAP}}^\dagger$ equivalence classes are the only perfect entanglers contained in three planes. Perfect entanglers with a chord passing through origin can transform a pair of orthonormal product states into maximally entangled states. However, not all the perfect entanglers without any chord passing through origin can transform a pair of orthonormal product states into maximally entangled states; only those satisfying one of the conditions derived in section IV can do such a transformation.

[1] A. Barenco, C.H. Bennett, R. Cleve, D.P. DiVincenzo, N. Margolus, P. Shor, T. Sleator, J.A. Smolin, H. Weinfurter, Phys. Rev. A 52(5), 3457 (1995).
[2] A. Barenco, Proc. R. Soc. Lond. A 449, 679–683 (1995).
[3] D.P. DiVincenzo, Phys. Rev. A 51(2), 1015 (1995).
[4] Y. Makhlin, Quantum Inf. Process. 1, 243 (2002).
[5] J. Zhang, J. Vala, S. Sastry, K.B. Whaley, Phys. Rev. A 67(4), 042313 (2003).
[6] P. Zanardi, Phys. Rev. A 63(4), 040304(R) (2001).
[7] M.A. Nielsen, C.M. Dawson, J.L. Dodd, A. Gilchrist, D. Mortimer, T.J. Osborne, M.J. Bremner, A.W. Harrow, A. Hines, Phys. Rev. A 67(5), 052301 (2003).
[8] P. Zanardi, C. Zalka, and L. Faoro, Phys. Rev. A 62(3), 030301(R) (2000).
[9] A. T. Rezakhani, Phys. Rev. A 70(5), 052313 (2004).

[10] S. Balakrishnan, and R. Sankaranarayanan, Phys. Rev. A 82(3), 034301 (2010).
[11] B. Jonnadula, P. Mandayam, K. Życzkowski, A. Lakshminarayan, Phys. Rev. A 95(4), 040302(R) (2017).
[12] B. Jonnadula, P. Mandayam, K. Życzkowski, A. Lakshminarayan, Phys. Rev. Res. 2(4), 043126 (2020).
[13] K. Selvan, and S. Balakrishnan, Eur. Phys. J. D 78(11), 137 (2024).
[14] A. Chefles, Phys. Rev. A 72(4), 042332 (2005).
[15] N. Yu, R. Duan, M. Ying, Phys. Rev. A 81(3), 032328 (2010).
[16] M. K. Selvan, and S. Balakrishnan, Phys. Scr. 99(3), 035113 (2024).
[17] K. Selvan, and S. Balakrishnan, Eur. Phys. J. D 77(7), 144 (2023).
[18] X. Wang, and P. Zanardi, Phys. Rev. A 66(4), 044303 (2002).
[19] S. Balakrishnan, and R. Sankaranarayanan, Phys. Rev. A 83(6), 062320 (2011).